Effects of chirality on single-file water permeability and diffusivity through single wall carbon nanotubes

Alireza R. Binesh[1], *Reza Kamali*[2] ✉

[1]*Malek-e-Ashtar University of Technology, Shiraz, Iran*
[2]*School of Mechanical Engineering, Shiraz University, Shiraz, 71348-51154, Iran*
✉ *E-mail: rkamali@shirazu.ac.ir*

Published in Micro & Nano Letters; Received on 10th June 2016; Revised on 16th September 2016; Accepted on 12th October 2016

In this work, molecular dynamics (MD) simulations of single-file water permeation through carbon nanotube (CNT) membranes have been performed and for a better understanding of the relationship between water transport performance of these biomimetic membranes and chirality of CNTs, the key parameters such as osmotic and diffusive permeability constants and diffusion coefficients are investigated. For this purpose, CNTs with approximately same diameters and different chirality from armchair to zigzag are used to perform 40 nanosecond MD simulations of these membranes. The resulting permeability and diffusivity characteristics of single-file CNT membranes showed that water permeability constant and diffusion coefficient increase by changing in the chirality of CNTs from armchair to zigzag, with approximately similar size in diameter. Finally, the presented results provide useful insights into the design of CNT water transporters with best performance.

1. Introduction: Classical fluid mechanics suggest that the work required to move fluid through nanoscale channels grows prohibitively large as channel radius decreases and therefore the energy required for nanoscale pumping mechanisms would be prohibitively high. In contrast, channels with slippery walls can overcome these restrictions and reduce power requirements. It has been shown that by scientist and researchers, carbon nanotube (CNT) membranes have a mechanism for dramatically enhanced fluid flow and this enhancement has been demonstrated both numerically [1–6] and experimentally [7–9]. Therefore CNTs offer an opportunity to mimic natural protein channels and can be used as biomimetic channels. These channels can have broad applications such as drug delivery, water purification, chemical separations, sensing and in nanofluidic and gating devices [8, 10, 11]. CNTs are hollow cylindrical tubes of carbon atoms that their smooth interior make ideal low-friction fluid flow. Fluids have been observed moving through CNTs at flowrates orders of magnitude faster than those predicted by traditional continuum fluid mechanics. Therefore, understanding such fast flow could provide the facility to design and control liquid transport.

CNTs are cylindrical tubes of carbon atoms covalently bonded in a lattice of hexagonal rings. A CNT can be visualised as a graphene sheet that has been rolled into a cylinder. The rolling up of the graphene sheet is described by the chiral vector as follow

$$\boldsymbol{C} = n\boldsymbol{a}_1 + m\boldsymbol{a}_2 \equiv (n, m) \tag{1}$$

where the positive integers n and m are the distances along the unit axes and are known as the chiral indices. The orientation at which the carbon hexagons are tiled onto the nanotube is described by the this chiral vector (n, m) [12]. Physical properties of CNTs depend on chiral indices. CNT(n, 0) and CNT(n, n) corresponds to zigzag and armchair types, respectively. Intermediate chiral vectors where $n \neq m$ and $m \neq 0$ are termed chiral CNTs.

Many researchers investigated water transport in CNTs using molecular dynamics (MD) simulations. These studies were performed to have better understanding on effect of CNTs size [13–18], diffusion mechanism [19–24], different fluids [25–28] etc.

As mentioned, the dynamics of water molecules in CNTs has been studied for many years, but a comprehensive understanding of CNT structural parameters effects such as chirality on water transport performance of these channels is not completed yet and several important problems still persist. In this Letter, the results of the first MD simulation of CNT membrane with different chirality and same diameter have been reported and the effects of chirality on most important parameters of single-file water permeation through these biomimetic channels have been investigated for the first time.

2. Methodology: The initial coordinates of CNTs were built using Carbon Nanostructure Builder Plugin of visual molecular dynamics [29]. The length of all CNTs was set about 18.4 Å similar to the length of single file constriction region of most of aquaporins. The generated CNT structures were embedded into two graphene sheets to reach a CNT membrane configuration similar to biological membranes. Finally, two slabs of water molecules were placed top and bottom of the CNT membrane. In all simulations periodic boundary conditions are applied in all directions. All presented MD simulations were performed with NAMD [30] at constant particle number, volume and temperature ensemble. Water molecules were modelled by the well-known TIP3P model [31]. Temperature was controlled at 300 Kelvin with a Langevin dynamics thermostat with a Langevin damping coefficient $\gamma = 5$ ps-1. The Particle Mesh Ewald method [32] was used for computing electrostatic interactions. The cut-off radius of van der Waals interactions is set to 12 Å. In all cases 40 nanosecond of equilibrium MD simulations were done using 1 fs time step.

3. Results and discussion: As already mentioned, this research was mainly focused on water permeability analysis of CNTs single file water transporters. For this purpose, the MD simulation of water transport through CNTs with different chirality and approximately same diameter were carried out in order to estimating of key parameters of these channels such as osmotic and diffusive permeability constants and diffusion coefficients.

To investigate the role of CNT chirality on water permeability of biomimetic channels, the MD simulations of five CNT membranes with different chiralities including CNT(6, 6), CNT(7, 5), CNT(8, 4), CNT(9, 2) and CNT(10, 1) have been performed. In Figs. 1 and 2 geometries of CNTs with different chiral angles were shown. As seen in these figures, these CNT membranes have same length (18.4 Å) and approximately same diameters. Snapshots of MD simulations of CNT membranes with different chiral angles were presented in Fig. 2. As shown, water single file

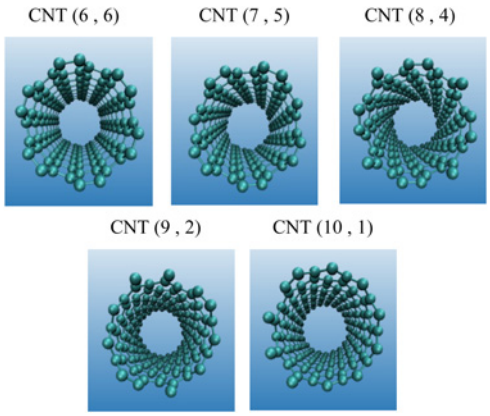

Fig. 1 *Geometry of CNTs with different chiral angles*

chain structure has been formed in all of CNT membranes with different chirality.

CNTs are one of the best candidates for efficient fluids transport due to their hydrophobic and molecularly smooth surfaces and water permeation through these nanoscale channels is similar to the biological channels water transport mechanism. MD simulation of single-file water transport through nanopores such as aquaporins and CNTs was proposed by Hummer *et al.* [1]. They described the statistics of water single-file transport based on a continuous time random walk (CTRW) model. In this model it is assumed that when a water molecule detaches the single file chain and left the channel, another water molecule quickly joins with the single file chain from the opposite end of the nanochannel. This process is known as a 'hop' of the single file chain. The channel is always filled by a fixed number of water molecules N^- that form the single file chain. Therefore, for a complete permeation event, N^-+1 hops must occur.

The CTRW model can give estimations for the diffusive and osmotic permeability coefficients, according to collective coordinate model that has been described in previous sections. Moreover, in the CTRW model the one-dimensional diffusion coefficient D can be calculated from bidirectional hopping rate k [33]

$$D = \frac{k \cdot a^2}{2} \tag{2}$$

where $a = 2.6$ Å is the average distance of neighbouring water molecules in a single file chain.

Moreover, on the basis of the CTRW model, the single-channel diffusive permeability constant p_d can be calculated from equilibrium MD simulation as follow [34, 35]

$$p_d = v_w \cdot q_0 \tag{3}$$

where v_w is the average volume of a single water molecule and q_0 is the number of water molecules which cross the CNT per unit time.

To osmotic permeability coefficient (p_f) calculation from equilibrium MD simulations the collective diffusion model proposed by Zhu *et al.* [36] was used. In this model, the normalise collective coordinate $n(t)$ is determined using the z-direction displacement of each water molecules that located at CNT single file during time step dt

$$dn(t) = \sum_{i \in S(t)} dz_i / L(t) \tag{4}$$

$$n(t) = \int dt/L \sum_{i \in S(t)} [z_i(t) - z_i(t - \delta t)], \quad \delta t = 1 \text{ ps} \tag{5}$$

where L is the CNT length, $S(t)$ is the set of water molecules inside the CNT at time t and δt is the time step size.

The collective diffusion constant is defined as follow, using Einstein relation

$$D_n = \langle n^2(t) \rangle / 2t \tag{6}$$

where $\langle n^2(t) \rangle$ is the mean square displacement (MSD) of $n(t)$. Finally the single file osmotic permeability constant (p_f) can be calculated as follow

$$p_f = v_w D_n \tag{7}$$

The collective coordinates $n(t)$ as function of simulation time and MSD of these collective coordinates averaging over 400 100-ps time windows were presented in Figs. 3 and 4, respectively. According to Fig. 4, the linear regression of collective coordinates

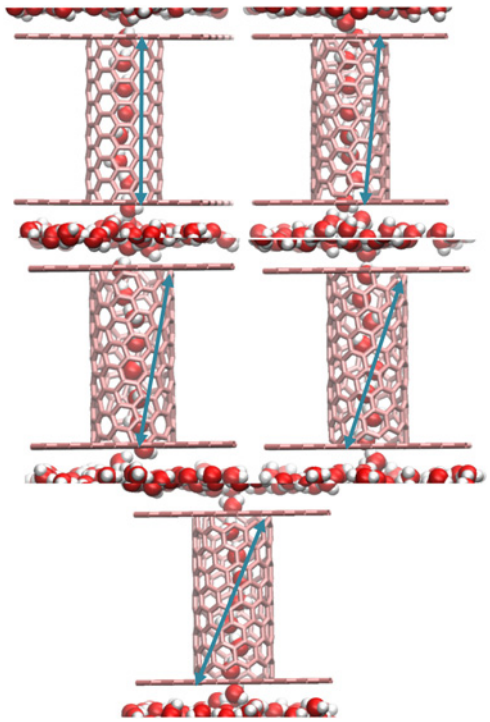

Fig. 2 *Snapshots of MD simulation of CNT membranes with different chiral angles*

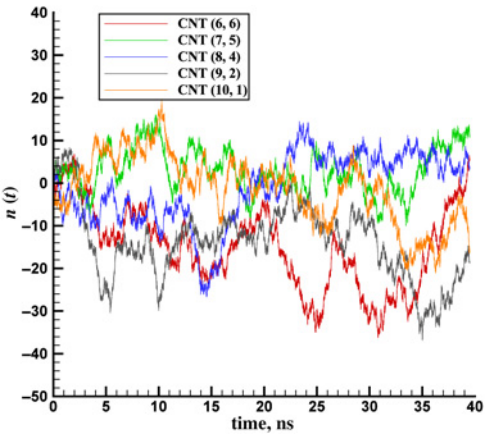

Fig. 3 *Collective coordination n(t) against simulation time for CNT membranes with different chiral angles*

doi: 10.1049/mnl.2016.0384

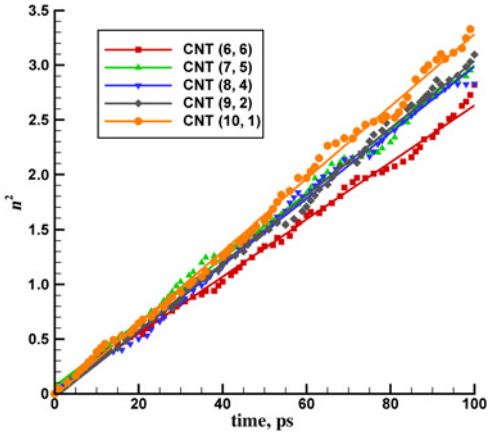

Fig. 4 *MSD of collective coordinates and linear regression of MSD curves for CNT membranes with different chiral angles*

Table 1 Summary of water permeability characteristics of CNT membranes with different chiralities

CNT	D, Å	Permeation events	q_0 (1/ns)	p_d	p_f	p_f/p_d	$\bar{N}$
(6, 6)	8.14	155	1.96	5.87	38.87	6.63	6.95
(7, 5)	8.17	183	2.32	6.93	43.80	6.32	6.87
(8, 4)	8.29	191	2.42	7.23	45.15	6.25	6.85
(9, 2)	7.95	199	2.52	7.53	46.05	6.11	6.74
(1, 10)	8.25	201	2.54	7.61	49.34	6.49	6.80

p_f and p_d units in 10^{-14} cm^3/s

MSD of chiral CNT(10, 1) has the maximum slope resulting in maximum osmotic water permeability and the linear regression slope of MSD of armchair CNT CNT(6, 6) collective coordinates is minimum resulting in minimum osmotic water permeability.

A summary of water permeability characteristics of CNT membranes with different chiralities has been presented in Table 1 and in Table 2. Diffusion coefficients of these armchair and chiral CNT membranes were calculated based on the described method. As shown in these tables, the minimum complete water permeation events occurred in armchair CNT(6, 6) and this parameter increases with chirality increment of CNT membranes.

It should be noted that, in order to estimate the single channel diffusive water permeability constant p_d, the number of water molecules that completely crossing the CNTs in both positive and negative directions along the CNTs were calculated during 40 ns of the MD simulations. The number of permeation events for each CNT is presented in Table 1. The number of water molecules which cross the channel unidirectionally per unit time (q_0) was determined and finally the diffusive water permeability constants of each CNT were obtained from (2).

The ratio of osmotic and diffusive permeability constants (p_f/p_d), presented in Table 1 is an important characteristics of water permeability through CNTs and in contrast to osmotic and diffusive

Table 2 Diffusion coefficient of CNT membranes with different chiralities

CNT	Permeation events	q_0 (1/ns)	Hopping rate k (1/ns)	D (10^{-5} cm^2/s)
(6, 6)	155	1.96	31.62	1.07
(7, 5)	183	2.32	37.78	1.28
(8, 4)	191	2.42	39.52	1.34
(9, 2)	199	2.52	41.83	1.41
(1, 10)	201	2.54	41.89	1.42

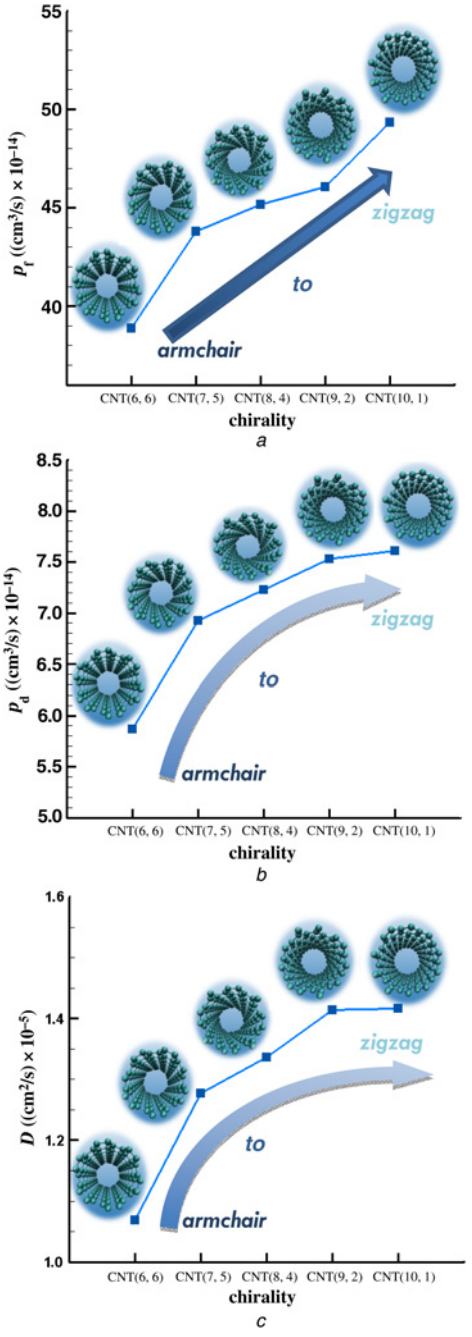

Fig. 5 *Variations of*
a Osmotic water permeability
b Diffusive water permeability
c Diffusion constant as function of the CNT chirality

permeability constants, this parameter can be measured experimentally for a channel without knowing the density of channels [37]. Based on CTRW model this ratio is related to the average occupancy number of water molecules in the channel as $p_f/p_d = N + 1$. Therefore, this ratio can be used as a measure of the 'single-fileness' of nanochannels and biomembranes. According to values of this ratio, the water permeation in all of these CNTs has pronounced single-file structure.

In Fig. 5 variations of osmotic water permeability constant, diffusive water permeability constant and diffusion coefficient as function of the CNT chirality is presented. As it is observed, these important parameters increase by changing in the chirality of CNTs from armchair to zigzag. Therefore, in CNT membranes with same length and diameter, water permeability and diffusivity can increase with the increase in chirality of CNT.

4. Conclusion: Effects of chirality on water permeability performance of CNT biomimetic channels have been investigated with a membrane thickness similar to the length of single file constriction region of most of aquaporins. From investigation of CNT chirality effect, it is observed that the minimum complete water permeation events occurred in armchair CNT(6, 6) and this parameter increases with chirality increment of CNT membranes and osmotic and diffusivity water permeability constant and diffusion coefficient increase by changing in the chirality of CNTs from armchair to zigzag. Moreover, from the ratio of osmotic and diffusive permeability constants, it is observed that the water permeation in all of investigated CNTs has single-file structure. The presented MD simulations results of single file water transport in armchair and chiral CNTs give useful insights to design and fabricate of biomimetic membranes and channels with best water permeability and diffusivity performance.

5 References

[1] Hummer G., Rasaiah J.C., Noworyta J.P.: 'Water conduction through the hydrophobic channel of a carbon nanotube', *Nature*, 2001, **414**, pp. 188–190

[2] Whitby M., Quirke N.: 'Fluid flow in carbon nanotubes and nanopipes', *Nat. Nanotechnol.*, 2007, **2**, pp. 87–94

[3] Noy A., Park H.G., Fornasiero F., *ET AL.*: 'Nanofluidics in carbon nanotubes', *Nano Today*, 2007, **2**, pp. 22–29

[4] Mattia D., Gogotsi Y.: 'Review: static and dynamic behavior of liquids inside carbon nanotubes', *Microfluidics Nanofluidics*, 2008, **5**, pp. 289–305

[5] Ritos K., Mattia D., Calabrò F., *ET AL.*: 'Flow enhancement in nanotubes of different materials and lengths', *J. Chem. Phys.*, 2014, **140**, p. 014702

[6] Thomas J.A., McGaughey A.J., Kuter-Arnebeck O.: 'Pressure-driven water flow through carbon nanotubes: insights from molecular dynamics simulation', *Int. J. Therm. Sci.*, 2010, **49**, pp. 281–289

[7] Holt J.K., Park H.G., Wang Y., *ET AL.*: 'Fast mass transport through sub-2-nanometer carbon nanotubes', *Science*, 2006, **312**, pp. 1034–1037

[8] Holt J.K., Noy A., Huser T., *ET AL.*: 'Fabrication of a carbon nanotube-embedded silicon nitride membrane for studies of nanometer-scale mass transport', *Nano Lett.*, 2004, **4**, pp. 2245–2250

[9] Majumder M., Chopra N., Andrews R., *ET AL.*: 'Nanoscale hydrodynamics: enhanced flow in carbon nanotubes', *Nature*, 2005, **438**, pp. 44–44

[10] Lopez C.F., Nielsen S.O., Moore P.B., *ET AL.*: 'Understanding nature's design for a nanosyringe', *Proc. Natl. Acad. Sci. USA*, 2004, **101**, pp. 4431–4434

[11] Gao Y., Bando Y.: 'Nanotechnology: Carbon nanothermometer containing gallium', *Nature*, 2002, **415**, pp. 599–599

[12] White C., Robertson D., Mintmire J.: 'Helical and rotational symmetries of nanoscale graphitic tubules', *Phys. Rev. B*, 1993, **47**, p. 5485

[13] Pascal T.A., Goddard W.A., Jung Y.: 'Entropy and the driving force for the filling of carbon nanotubes with water', *Proc. Natl. Acad. Sci.*, 2011, **108**, pp. 11794–11798

[14] Srivastava R., Docherty H., Singh J.K., *ET AL.*: 'Phase transitions of water in graphite and mica pores', *J. Phys. Chem. C*, 2011, **115**, pp. 12448–12457

[15] Ye H., Zhang H., Zheng Y., *ET AL.*: 'Nanoconfinement induced anomalous water diffusion inside carbon nanotubes', *Microfluidics Nanofluidics*, 2011, **10**, pp. 1359–1364

[16] Mashl R.J., Joseph S., Aluru N., *ET AL.*: 'Anomalously immobilized water: a new water phase induced by confinement in nanotubes', *Nano Lett.*, 2003, **3**, pp. 589–592

[17] Liu Y., Wang Q., Wu T., *ET AL.*: 'Fluid structure and transport properties of water inside carbon nanotubes', *J. Chem. Phys.*, 2005, **123**, p. 234701

[18] Liu Y., Wang Q., Zhang L., *ET AL.*: 'Dynamics and density profile of water in nanotubes as one-dimensional fluid', *Langmuir*, 2005, **21**, pp. 12025–12030

[19] Barati Farimani A., Aluru N.: 'Spatial diffusion of water in carbon nanotubes: from fickian to ballistic motion', *J. Phys. Chem. B*, 2011, **115**, pp. 12145–12149

[20] Mukherjee B., Maiti P.K., Dasgupta C., *ET AL.*: 'Strongly anisotropic orientational relaxation of water molecules in narrow carbon nanotubes and nanorings', *ACS Nano*, 2008, **2**, pp. 1189–1196

[21] Das A., Jayanthi S., Deepak H.S.M.V., *ET AL.*: 'Single-file diffusion of confined water inside SWNTs: an NMR study', *ACS Nano*, 2010, **4**, pp. 1687–1695

[22] Striolo A.: 'The mechanism of water diffusion in narrow carbon nanotubes', *Nano Lett.*, 2006, **6**, pp. 633–639

[23] Martı J., Gordillo M.: 'Microscopic dynamics of confined supercritical water', *Chem. Phys. Lett.*, 2002, **354**, pp. 227–232

[24] Kamali R., Binesh A.: 'A comparison of neural networks and adaptive neuro-fuzzy inference systems for the prediction of water diffusion through carbon nanotubes', *Microfluidics Nanofluidics*, 2013, **14**, pp. 575–581

[25] Supple S., Quirke N.: 'Rapid imbibition of fluids in carbon nanotubes', *Phys. Rev. Lett.*, 2003, **90**, p. 214501

[26] Supple S., Quirke N.: 'Molecular dynamics of transient oil flows in nanopores I: imbibition speeds for single wall carbon nanotubes', *J. Chem. Phys.*, 2004, **121**, pp. 8571–8579

[27] Supple S., Quirke N.: 'Molecular dynamics of transient oil flows in nanopores. II. Density profiles and molecular structure for decane in carbon nanotubes', *J. Chem. Phys.*, 2005, **122**, pp. 104706–104706

[28] Kalra A., Hummer G., Garde S.: 'Methane partitioning and transport in hydrated carbon nanotubes', *J. Phys. Chem. B*, 2004, **108**, pp. 544–549

[29] Humphrey W., Dalke A., Schulten K.: 'VMD: visual molecular dynamics', *J. Mol. Graph.*, 1996, **14**, pp. 33–38

[30] Phillips J.C., Braun R., Wang W., *ET AL.*: 'Scalable molecular dynamics with NAMD', *J. Comput. Chem.*, 2005, **26**, pp. 1781–1802

[31] Jorgensen W.L., Chandrasekhar J., Madura J.D., *ET AL.*: 'Comparison of simple potential functions for simulating liquid water', *J. Chem. Phys.*, 1983, **79**, pp. 926–935

[32] Essmann U., Perera L., Berkowitz M.L., *ET AL.*: 'A smooth particle mesh Ewald method', *J. Chem. Phys.*, 1995, **103**, pp. 8577–8593

[33] Berezhkovskii A., Hummer G.: 'Single-file transport of water molecules through a carbon nanotube', *Phys. Rev. Lett.*, 2002, **89**, p. 064503

[34] Tajkhorshid E., Zhu F., Schulten K.: 'Kinetic theory and simulation of single-channel water transport', in Yip S. (Ed.): 'Handbook of materials modeling' (Springer, 2005), pp. 1797–1822

[35] Zhu F., Tajkhorshid E., Schulten K.: 'Theory and simulation of water permeation in aquaporin-1', *Biophys. J.*, 2004, **86**, pp. 50–57

[36] Zhu F., Tajkhorshid E., Schulten K.: 'Collective diffusion model for water permeation through microscopic channels', *Phys. Rev. Lett.*, 2004, **93**, p. 224501

[37] Mori S., Mathai J., Preston G., *ET AL.*: 'Functional analysis of aquaporin-1 deficient red cells', *J. Biol. Chem.*, 1996, **271**, pp. 1309–1313

doi: 10.1049/mnl.2016.0384